J|A|C|S
ARTICLES
Published on Web 08/18/2007

Phosphate-Mediated Arginine Insertion into Lipid Membranes and Pore Formation by a Cationic Membrane Peptide from Solid-State NMR

Ming Tang,[†] Alan J. Waring,[‡] and Mei Hong*,[†]

Contribution from the Department of Chemistry, Iowa State University, Ames, Iowa 50011, and Department of Medicine, University of California at Los Angeles School of Medicine, Los Angeles, California 90095

Received April 11, 2007; E-mail: mhong@iastate.edu

Abstract: The insertion of charged amino acid residues into the hydrophobic part of lipid bilayers is energetically unfavorable yet found in many cationic membrane peptides and protein domains. To understand the mechanism of this translocation, we measured the $^{13}C-^{31}P$ distances for an Arg-rich β-hairpin antimicrobial peptide, PG-1, in the lipid membrane using solid-state NMR. Four residues, including two Arg's, scattered through the peptide were chosen for the distance measurements. Surprisingly, all residues show short distances to the lipid ^{31}P: 4.0−6.5 Å in anionic POPE/POPG membranes and 6.5−8.0 Å in zwitterionic POPC membranes. The shortest distance of 4.0 Å, found for a guanidinium Cζ at the β-turn, suggests N−H···O−P hydrogen bond formation. Torsion angle measurements of the two Arg's quantitatively confirm that the peptide adopts a β-hairpin conformation in the lipid bilayer, and gel-phase ^1H spin diffusion from water to the peptide indicates that PG-1 remains transmembrane in the gel phase of the membrane. For this transmembrane β-hairpin peptide to have short $^{13}C-^{31}P$ distances for multiple residues in the molecule, some phosphate groups must be embedded in the hydrophobic part of the membrane, with the local ^{31}P plane parallel to the β-strand. This provides direct evidence for toroidal pores, where some lipid molecules change their orientation to merge the two monolayers. We propose that the driving force for this toroidal pore formation is guanidinium−phosphate complexation, where the cationic Arg residues drag the anionic phosphate groups along as they insert into the hydrophobic part of the membrane. This phosphate-mediated translocation of guanidinium ions may underlie the activity of other Arg-rich antimocrobial peptides and may be common among cationic membrane proteins.

Introduction

Charged and polar residues are surprisingly common in a diverse range of membrane proteins. For instance, cationic antimicrobial peptides (AMPs) such as protegrin-1 (PG-1: **R**GG**R**LCYC**RRR**FCVCVG**R**) permeabilize the lipid membranes of microbes to cause cell death.[1,2] Cell-penetrating peptides such as the HIV TAT peptide (48−60: G**RKKRR**Q**RRR**PPQ) are rich in Arg and Lys and yet translocate across cell membranes with ease.[3,4] Voltage-gated potassium channels contain voltage-sensing domains (e.g., KvAP S4 helix: LGLF**R**LV**R**LL**R**FL**R**ILLII) rich in Arg.[5] Polar residues such as Asn and Glu play important functional and stabilizing roles in the folding of membrane proteins by forming interhelical hydrogen bonds.[6−8] Generally, the insertion of the charged and polar residues into the hydrophobic part of the bilayer is energetically unfavorable. This has been studied in detail by measuring, for example, the free energies of transferring peptides from water to octanol.[9] However, this view is recently modified by the finding that hydrophobic residues compensate for the energy cost of incorporating charged and polar residues into the lipid bilayer and that the free energy of insertion also depends sensitively on the position of the polar residues in the membrane.[10] Using an *in vitro* endoplasmic reticulum translocon system, von Heijne, White, and co-workers measured the equilibrium constant of membrane insertion of designed polypeptides containing the amino acid of interest at various positions.[10] The resulting biological hydrophobicity scale for the 20 amino acids was found to be position-dependent as well as charge- and polarity- dependent. It was found that the S4 helix of the voltage-gated potassium channel KvAP inserts into the mem-

[†] Iowa State University.
[‡] University of California at Los Angeles School of Medicine.

(1) Bellm, L.; Lehrer, R. I.; Ganz, T. *Exp. Opin. Invest. Drugs* **2000**, *9*, 1731−1742.
(2) Hancock, R. E.; Lehrer, R. *Trends Biotechnol.* **1998**, *16*, 82−8.
(3) Vives, E.; Brodin, P.; Lebleu, B. *J. Biol. Chem.* **1997**, *272*, 16010−7.
(4) Jarver, P.; Langel, U. *Biochim. Biophys. Acta* **2006**, *1758*, 260−3.
(5) Long, S. B.; Campbell, E. B.; Mackinnon, R. *Science* **2005**, *309*, 897−903.
(6) DeGrado, W. F.; Gratkowski, H.; Lear, J. D. *Protein Sci.* **2003**, *12*, 647−65.
(7) Choma, C.; Gratkowski, H.; Lear, J. D.; DeGrado, W. F. *Nat. Struct. Biol.* **2000**, *7*, 161−166.
(8) Lear, J. D.; Gratkowski, H.; Adamian, L.; Liang, J.; DeGrado, W. F. *Biochemistry* **2003**, *42*, 6400−7.
(9) White, S. H.; Wimley, W. C. *Annu. Rev. Biophys. Biomol. Struct.* **1999**, *28*, 319−365.
(10) Hessa, T.; Kim, H.; Bihlmaier, K.; Lundin, C.; Boekel, J.; Andersson, H.; Nilsson, I.; White, S. H.; von Heijne, G. *Nature* **2005**, *433*, 377−81.

10.1021/ja072511s CCC: $37.00

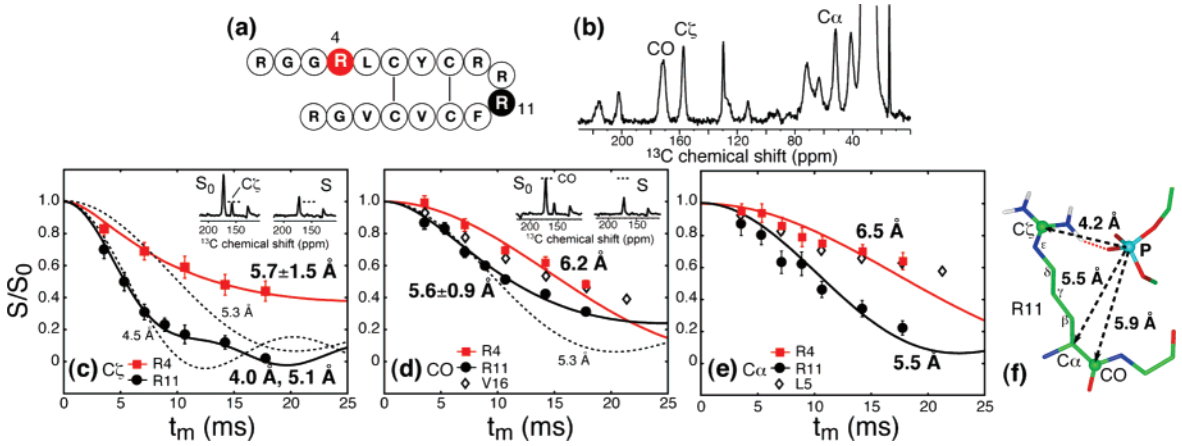

Figure 1. $^{13}C-^{31}P$ REDOR data of Arg_4 (red squares), Arg_{11} (black circles), Leu_5 and Val_{16} (open diamonds) of PG-1 in POPE/POPG membranes. (a) Amino acid sequence of PG-1. The labeled Arg_4 and Arg_{11} are shaded. (b) ^{13}C spectrum of Arg_4 in the TRE-POPE/POPG membrane. The assigned Arg peaks are resolved from the lipid ^{13}C signals. (c) $^{13}C\zeta-^{31}P$ distances of Arg_4 and Arg_{11}. Best-fit distances are 5.7 ± 1.5 Å for Arg_4 and 4.0 Å and 5.1 Å (1:1) for Arg_{11}. The single-distance best-fit curves of 5.3 Å and 4.5 Å (dashed lines) disagree with the experiment, indicating a distance distribution for Arg_{11}. A pair of REDOR spectra of Arg_{11} Cζ is shown in the inset. (d) $^{13}CO-^{31}P$ distances. Best-fit distances are 6.2 Å for Arg_4 and Val_{16} and 5.6 ± 0.9 Å for Arg_{11}. The single-distance curve of 5.3 Å (dashed line) does not fit the Arg_{11} data. A pair of Arg_{11} REDOR spectra is shown in the inset. (e) $^{13}C\alpha-^{31}P$ distances. Best-fit distances are 6.3 Å for Arg_4 and Leu_5 and 5.5 Å for Arg_{11}. (f) Model of the guanidinium−phosphate complex for Arg_{11} with the measured $^{13}C-^{31}P$ distances. A putative hydrogen bond between the guanidinium and phosphate groups is indicated as a red dotted line.

brane despite the presence of four Arg's,[11] and the fraction of insertion increases when two Arg residues moved one step closer to the C-terminus. Molecular dynamics simulations showed that the effective lipid bilayer thickness was reduced to an astonishingly small ~10 Å near the inserted S4 helix so that water and phosphate groups stabilize the Arg residues in the middle of the helix through hydrogen bonding.[12] However, such a dramatic accommodation of the Arg residues by the lipid bilayer has not been directly observed experimentally.

PG-1 is a broad-spectrum AMP found in porcine leukocytes.[1,13] It is a β-hairpin molecule stabilized by two disulfide bonds and contains six Arg residues (Figure 1a). Its Arg-rich sequence and β-sheet conformation[14] are characteristic of many AMPs such as human defensins and tachyplesin.[15,16] PG-1 carries out its antimicrobial function by forming pores in the microbial cell membrane, thus disrupting the membrane's barrier function. These pores were observed from lipid vesicle leakage assays[17,18] and neutron diffraction.[19] Recently, ^1H and ^{19}F spin diffusion NMR data showed that PG-1 self-assembles into a transmembrane oligomeric β-barrel in bacteria-mimetic POPE/POPG membranes,[20] providing the first high-resolution structure of PG-1 at the pores. However, the depths of insertion of the Arg residues in these β-barrels relative to the lipid bilayer remain elusive. According to the hydrophobicity scale of White and Von Heijne, the insertion of a single Arg into the center of the bilayer costs a free energy of 2.58 kcal/mol,[10] one of the highest ΔG values among the 20 amino acids. Yet PG-1, with six Arg residues distributed both in the middle of the β-strand and at the two ends of the β-hairpin, has been shown to insert well into the hydrophobic part of most lipid membranes except for cholesterol-containing POPC bilayers at high peptide concentrations.[20−23] To solve this puzzle, we have now measured the distances between Arg residues in PG-1 and ^{31}P of the lipid headgroups using rotational-echo double resonance (REDOR) experiments. Surprisingly, we found that both Arg's at the β-turn and in the middle of the β-strand have short distances of less than 6.5 Å to ^{31}P. This is true for both the backbone and the side chain of the Arg residues, and thus side chain snorkeling to the membrane surface[24] cannot account for the observation. Instead, the data indicate that PG-1 causes some of the phosphate groups to insert into the hydrophobic part of the membrane so that the local ^{31}P plane is parallel to the β-strands. Thus, some lipid molecules must change their orientations and merge the two monolayers, as proposed in the toroidal pore model. These results, which represent the first high-resolution distance constraints of Arg residues in proteins with respect to lipid membranes, suggest that the molecular mechanism for toroidal pore formation is guanidinium−phosphate complexation, which neutralizes the guanidinium ions before they are inserted into the membrane.

Materials and Methods

All lipids were purchased from Avanti Polar Lipids (Alabaster, AL). PG-1 was synthesized using Fmoc chemistry as previously described.[25] Four PG-1 samples were synthesized, containing U-^{13}C,^{15}N-Arg_4 and ^{15}N-Leu_5, U-^{13}C,^{15}N-Arg_{11} and ^{15}N-Phe_{12}, $^{13}C\alpha$-Leu_5, and ^{13}CO-Val_{16}. U-^{13}C,^{15}N-labeled Arg was obtained from Spectra Stable Isotopes (Columbia, MD) as Fmoc-Arg(MTR)-OH.

(11) Hessa, T.; White, S. H.; von Heijne, G. *Science* **2005**, *307*, 1427.
(12) Freites, J. A.; Tobias, D. J.; von Heijne, G.; White, S. H. *Proc. Natl. Acad. Sci. U.S.A.* **2005**, *102*, 15059−64.
(13) Kokryakov, V. N.; Harwig, S. S.; Panyutich, E. A.; Shevchenko, A. A.; Aleshina, G. M.; Shamova, O. V.; Korneva, H. A.; Lehrer, R. I. *FEBS Lett.* **1993**, *327*, 231−6.
(14) Fahrner, R. L.; Dieckmann, T.; Harwig, S. S.; Lehrer, R. I.; Eisenberg, D.; Feigon, J. *Chem. Biol.* **1996**, *3*, 543−550.
(15) Hancock, R. E.; Scott, M. G. *Proc. Natl. Acad. Sci. U.S.A.* **2000**, *97*, 8856−8861.
(16) Zasloff, M. *Nature* **2002**, *415*, 389−395.
(17) Ternovsky, V. I.; Okada, Y.; Sabirov, R. Z. *FEBS Lett.* **2004**, *576*, 433−6.
(18) Lehrer, R. I.; Barton, A.; Ganz, T. *J. Immunol. Methods* **1988**, *108*, 153−8.
(19) Yang, L.; Weiss, T. M.; Lehrer, R. I.; Huang, H. W. *Biophys. J.* **2000**, *79*, 2002−9.
(20) Mani, R.; Cady, S. D.; Tang, M.; Waring, A. J.; Lehrer, R. I.; Hong, M. *Proc. Natl. Acad. Sci. U.S.A.* **2006**, *103*, 16242−16247.
(21) Buffy, J. J.; Waring, A. J.; Lehrer, R. I.; Hong, M. *Biochemistry* **2003**, *42*, 13725−13734.
(22) Buffy, J. J.; Hong, T.; Yamaguchi, S.; Waring, A.; Lehrer, R. I.; Hong, M. *Biophys. J.* **2003**, *85*, 2363−2373.
(23) Heller, W. T.; Waring, A. J.; Lehrer, R. I.; Huang, H. W. *Biochemistry* **1998**, *37*, 17331−8.
(24) Segrest, J. P.; De Loof, H.; Dohlman, J. G.; Brouillette, C. G.; Anantharamaiah, G. M. *Proteins* **1990**, *8*, 103−17.
(25) Yamaguchi, S.; Hong, T.; Waring, A.; Lehrer, R. I.; Hong, M. *Biochemistry* **2002**, *41*, 9852−9862.

POPE and POPG lipids were mixed in chloroform at a 3:1 molar ratio and blown dry under N_2 gas. The mixture was then redissolved in cyclohexane and lyophilized. The dry lipid powder was dissolved in water and subjected to five cycles of freeze−thawing to form uniform vesicles. An appropriate amount of PG-1 to reach a peptide−lipid molar ratio of 1:12.5 was dissolved in water and mixed with the lipid vesicle solution, incubated at 303 K overnight, then centrifuged at 55 000 rpm for 2.5 h. The pellet was packed into an MAS rotor, giving a hydrated membrane sample. For the trehalose-protected membrane samples, the pellet was resuspended in water, and an amount of trehalose equivalent to 20% of the dry mass of the lipid and peptide was added.[26] The suspension was subjected to three freeze−thawing cycles, then lyophilized and packed into a rotor. A further lyophilization step was applied to the sample in the rotor to remove moisture gained during packing. The POPC samples were prepared similarly. The sugar-protected dry membranes have the same lamellar structure as hydrated membranes but have reduced lipid headgroup motion, thus enabling distance experiments to be conducted at mild temperatures.[27]

NMR experiments were carried out on a Bruker DSX-400 (9.4 T) spectrometer (Karlsruhe, Germany) and an AVANCE II 600 MHz (14.1 T) spectrometer. Triple-resonance magic-angle spinning (MAS) probes with a 4 mm spinning module was used. Low temperatures were reached using a Kinetics Thermal Systems XR air-jet sample cooler (Stone Ridge, NY) on the 400 MHz system and a Bruker BCU-Xtreme unit on the 600 MHz spectrometer. Typical 90° pulse lengths were 4−5 μs for ^{13}C and ^{31}P, and ^{1}H decoupling fields of 50−80 kHz were used. ^{13}C chemical shifts were referenced externally to the α-Gly ^{13}C′ signal at 176.49 ppm on the TMS scale.

^{13}C−^{31}P distances were measured using a selective REDOR experiment[28] for the uniformly ^{13}C,^{15}N-labeled Arg residues and nonselective REDOR[29] for the site-specifically labeled Leu_5 ^{13}Cα and Val_{16} ^{13}CO samples. Composite 90°180°90° pulses were applied on the ^{31}P channel to reduce the effect of flip angle errors and enhance the distance accuracy.[30] For the selective REDOR experiment, the central ^{13}C π pulse is a rotor-synchronized Gaussian pulse of 444 or 888 μs centered at the ^{13}C frequency of interest. This soft pulse recouples the desired ^{13}C−^{31}P dipolar coupling but removes the ^{13}C−^{13}C *J*-coupling between the ^{13}C on resonance and its directly bonded ^{13}C. For the specifically labeled samples, a hard ^{13}C π pulse was used. At each REDOR mixing time (t_m), a control experiment (S_0) with the ^{31}P pulses off and a dephasing experiment (S) with the ^{31}P pulses on were carried out. The normalized dephasing, S/S_0, as a function of t_m gives the ^{13}C−^{31}P dipolar coupling. The CO data were corrected for the lipid natural-abundance CO signal. The experiments were conducted under 4.5 kHz MAS at 253 K for the TRE-POPE/POPG membranes and under 5 kHz MAS and 263 K for the TRE-POPC membranes. ^{31}P 180° pulse lengths of 8−9 μs were used to achieve complete inversion of the broad ^{31}P resonance.

The ψ angles of Arg_4 and Arg_{11} were measured using the NCCN technique, which correlates the $^{15}N_i$−$^{13}C\alpha_i$ and $^{13}CO_i$−$^{15}N_{i+1}$ dipolar couplings to obtain the relative orientation of the two bonds.[31,32] ^{13}Cα−^{13}CO double quantum coherence was excited using the SPC-5 sequence[33] and evolves under the REDOR-recoupled ^{13}C−^{15}N dipolar interaction.[29] A pair of ^{13}C spectra were collected at each C−N mixing time, and the S/S_0 values of the CO and Cα signals were averaged and plotted as a function of mixing time to yield the ψ-angle dependent curve. The ϕ angles were measured using the HNCH technique, which correlates the $^1H^N$−^{15}N and ^{13}Cα−^{1}Hα dipolar couplings.[34] The experiment yields the H^N−N−Cα−Hα angle (ϕ_H), which is related to the ϕ-angle according to $\phi = \phi_H + 60°$. The NCCN and HNCH experiments were conducted at 253 K on the trehalose-protected membrane samples under 5.5 kHz and 4.44 kHz MAS, respectively.

The 2D ^{31}P−^{1}H correlation experiment with ^{1}H spin diffusion[35] was conducted on hydrated POPE/POPG membranes with and without PG-1 at 303 K under 5 kHz MAS. The ^{1}H spin diffusion mixing time was 64 ms, and a pre-evolution ^{1}H T_2 filter of 800 μs was used to select the mobile component. The ^{1}H−^{31}P CP contact time was 4 ms. The ^{1}H chemical shifts of the POPE/POPG membrane were assigned via the well-known ^{13}C chemical shifts by a ^{13}C−^{1}H 2D correlation experiment.

The gel-phase ^{1}H spin diffusion experiment[36] from water to peptide was carried out on DLPC-bound PG-1 samples, which were used previously to measure the depths of PG-1 residues in the liquid-crystalline (LC) phase by Mn^{2+} paramagnetic relaxation enhancement.[22] The experiments were performed between 230 and 243 K, such that the water ^{1}H line width after a 200 μs T_2 filter is 330 Hz.[37] After the T_2 filter, only the water ^{1}H magnetization and a small amount of headgroup γ proton signal remains, so that, without spin diffusion, the ^{13}C spectrum suppresses all peptide and lipid signals except for the lipid Cγ signal. ^{1}H mixing times of 0.25−49 ms were then used to detect peptide signals that result from spin diffusion from the membrane surface water.

Table 1. ^{13}C Isotropic Chemical Shifts (δ) and Full Width Half-Maximum (FWHM) Linewidths of Arg_4 and Arg_{11} in Trehalose-Protected POPE/POPG and POPC Membranes

		POPE/POPG		POPC	
		δ	fwhm	δ	fwhm
residue	site	(ppm)	(ppm)	(ppm)	(ppm)
Arg_4	CO	171.0	4.5	171.1	5.1
	Cα	51.7	3.5	51.7	4.2
	Cζ	157.2	2.6	157.2	2.9
Arg_{11}	CO	172.1	3.8	173.1	4.2
	Cα	53.3, 54.3	6.6	53.8	5.8
	Cζ	157.4	2.5	157.3	2.6

Results

^{13}C−^{31}P Distances between PG-1 and Lipid Headgroups. We measured the distances from two Arg residues, Arg_4 and Arg_{11}, and two hydrophobic residues, Leu_5 and Val_{16}, to the lipid phosphate groups. Arg_{11} represents the β-turn, which contains three consecutive Arg's, whereas Arg_4 lies in the middle of the N-terminal β-strand (Figure 1a). Two types of lipid membranes were used to bind the peptide: the anionic POPE/POPG mixture mimics the bacterial membrane, whereas the zwitterionic POPC bilayer allows the electrostatic effect on distances to be examined. Figure 1b shows a representative ^{13}C spectrum of Arg_4 in trehalose-protected POPE/POPG (TRE-POPE/POPG) membrane. Both Arg_4 and Arg_{11} exhibit β-sheet secondary shifts for Cα and CO (Table 1), but the Arg_4 Cα chemical shift is smaller than that for Arg_{11} Cα, indicating a more ideal β-sheet conformation. The Arg Cβ peak overlaps with Cγ (Figure S1) and thus cannot be used for secondary structure analysis. Arg_{11} Cα shows two peaks that are 1.0 ppm

(26) Crowe, J. H.; Crowe, L. M.; Chapman, D. *Science* **1984**, *223*, 701−703.
(27) Tang, M.; Waring, A. J.; Hong, M. *J. Magn. Reson.* **2006**, *184*, 222−227.
(28) Jaroniec, C. P.; Tounge, B. A.; Rienstra, C. M.; Herzfeld, J.; Griffin, R. G. *J. Am. Chem. Soc.* **1999**, *121*, 10237−10238.
(29) Gullion, T.; Schaefer, J. *J. Magn. Reson.* **1989**, *81*, 196−200.
(30) Sinha, N.; Schmidt-Rohr, K.; Hong, M. *J. Magn. Reson.* **2004**, *168*, 358−65.
(31) Costa, P. R.; Gross, J. D.; Hong, M.; Griffin, R. G. *Chem. Phys. Lett.* **1997**, *280*, 95−103.
(32) Feng, X.; Lee, Y. K.; Sandstroem, D.; Eden, M.; Maisel, H.; Sebald, A.; Levitt, M. H. *Chem. Phys. Lett.* **1996**, *257*, 314−320.
(33) Hohwy, M.; Rienstra, C. M.; Jaroniec, C. P.; Griffin, R. G. *J. Chem. Phys.* **1999**, *110*, 7983−7992.
(34) Hong, M.; Gross, J. D.; Griffin, R. G. *J. Phys. Chem. B* **1997**, *101*, 5869−5874.
(35) Huster, D.; Yao, X. L.; Hong, M. *J. Am. Chem. Soc.* **2002**, *124*, 874−883.
(36) Kumashiro, K. K.; Schmidt-Rohr, K.; Murphy, O. J.; Ouellette, K. L.; Cramer, W. A.; Thompson, L. K. *J. Am. Chem. Soc.* **1998**, *120*, 5043−5051.
(37) Gallagher, G. J.; Hong, M.; Thompson, L. K. *Biochemistry* **2004**, *43*, 7899−7906.

Table 2. $^{13}C-^{31}P$ Distances (Å) of PG-1 in POPE/POPG and POPC Membranes[a]

residue	site	POPE/POPG	POPC
Arg_4	Cζ	5.7 ± 1.5[b]	8.0
	Cα	6.5	-
	CO	6.2	7.2
Arg_{11}	Cζ	4.0, 5.1	6.5
	Cα	5.5	-
	CO	5.6 ± 0.9[b]	6.5
Leu_5	Cα	6.5	-
Val_{16}	CO	6.2	-

[a] For nondistributed distances the estimated uncertainties are 0.2 Å. [b] "±" denotes the half-width half-maximum of a Gaussian distance distribution.

apart, which we attribute to small conformational differences due to binding to two different lipid headgroups. Overall, the Arg chemical shifts are similar between the POPE/POPG membrane and the POPC membrane, indicating that the conformation is unchanged by the membrane composition.

Figure 1c−e shows the $^{13}C\{^{31}P\}$ REDOR data of various ^{13}C sites in the POPE/POPG membrane. At 253 K, the trehalose-protected membrane[27] has fully immobilized lipid headgroups, as manifested by the rigid-limit ^{31}P chemical shift span (193 ppm). A selective ^{13}C π pulse was used during the REDOR period for the Arg-labeled samples to remove the $^{13}C-^{13}C$ *J*-couplings.[28] Intriguingly, all backbone sites of the four residues as well as the side chain of both Arg residues gave short distances of 4.0−6.5 Å, with Arg_{11} Cζ exhibiting the shortest distances of 4.0 Å and 5.1 Å at a 1:1 ratio (Figure 1c). The backbone of the two hydrophobic residues has distances of 6.2 Å and 6.5 Å. These distances have estimated uncertainties of ±0.2 Å. In addition to the short distances, all REDOR curves show nearly quantitative (90%) decay, with the remaining 10% due to pulse imperfections.[30] This means that all peptides, rather than just a fraction, lie close to the lipid headgroups. To verify that the experiment can detect longer $^{13}C-^{31}P$ distances, we measured the intramolecular $^{13}C-^{31}P$ distances of POPE bilayers at 226 K. Indeed long distances of 8 Å and greater than 12 Å, which gave no detectable dephasing within a mixing time of 20 ms, were found for the lipid chain carbons far away from ^{31}P (Supporting Information Figure S2).

The above distances were extracted by fitting the experimental REDOR dephasing using a two-spin model. While in principle each ^{13}C spin can couple to multiple ^{31}P spins in the plane of the lipid bilayer, the large $^{31}P-^{31}P$ separation of ∼10 Å due to the size of the headgroups, combined with the strong $^{13}C-^{31}P$ dephasing observed for the PG-1 residues, results in a situation where the vertical distance from the ^{13}C to the multi-^{31}P plane is either the same as or slightly shorter than the two-spin distance. Thus, it is sufficient to analyze the measured REDOR data using the two-spin model. Importantly, the *relative* proximity of various ^{13}C labels to the ^{31}P spins are independent of whether two-spin or multispin models are used in the simulation. Detailed geometric consideration and numerical simulations for up to five-spin systems are given in the Supporting Information Figure S3.

While the distances between PG-1 and the lipid ^{31}P are overall short, there are residue-specific differences. Arg_{11} is closer to the ^{31}P than Arg_4 by 0.6−1.7 Å (Table 2). In particular, the short Arg_{11} Cζ−P distances (4.0 Å and 5.1 Å) suggest the formation of a guanidinium−phosphate complex through electrostatic interaction and hydrogen bonding. Figure 1f shows a model of this complex. The presence of two Arg_{11} Cζ−P distances is attributed to differential binding of the peptide to the zwitterionic POPE and anionic POPG lipids: the shorter 4.0 Å distance is most likely associated with the POPG fraction. This hypothesis is consistent with the presence of two slightly different Cα chemical shifts of Arg_{11} in the POPE/POPG membrane. Figure 1 also shows that the Arg_4 Cζ and Arg_{11} CO data do not match single-distance REDOR curves but require fitting by a Gaussian distance distribution, with half-width at half-maximum of 1.5 Å and 0.9 Å, respectively, suggesting conformational heterogeneity at these sites.

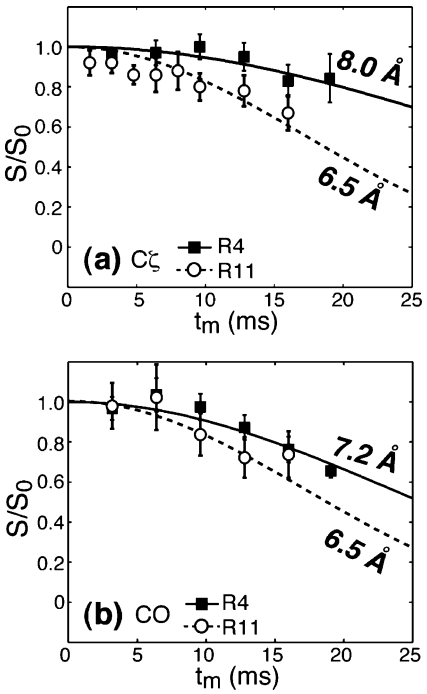

Figure 2. $^{13}C-^{31}P$ REDOR data of (a) Cζ and (b) CO of Arg_4 (■) and Arg_{11} (○) in POPC membrane, acquired at 263 K. (a) Best-fit Cζ−P distances are 8.0 Å for Arg_4 (solid line) and 6.5 Å for Arg_{11} (dashed line). (b) Best-fit CO−P distances are 7.2 Å for Arg_4 and 6.5 Å for Arg_{11}.

To further determine whether the Arg_4 and Arg_{11} distances to ^{31}P depend on the nature of the lipid headgroup, we measured the $^{13}C-^{31}P$ distances in the zwitterionic POPC membrane. Figure 2 shows that the distances are 1.0−2.5 Å longer in the POPC membrane than in the POPE/POPG membrane (Table 2). Thus, electrostatic attraction plays a significant role in the Arg−phosphate distances. Similar to the trend observed in the POPE/POPG membrane, Arg_4 is ∼1.0 Å further away from ^{31}P than Arg_{11} in the POPC membrane.

The peptide−lipid $^{13}C-^{31}P$ distances measured in the dry TRE-POPE/POPG membrane show only small differences from those in the hydrated POPE/POPG membrane. As shown in Figure S4, the Arg_4 Cζ−P distance increased from 5.7 ± 1.5 Å in the dry membrane to 6.8 Å in the hydrated membrane, whereas the Arg_{11} Cζ−P distance remained unchanged. The CO−P distances of both Arg's are 0.3−0.6 Å longer in the hydrated membrane. We attribute the small increase in $^{13}CO-^{31}P$ distances to residual motions in the hydrated membrane. This is confirmed by the slightly smaller ^{31}P chemical shift span of the hydrated membrane (184 ppm) at 226 K than that of the dry membrane at 253 K (193 ppm).

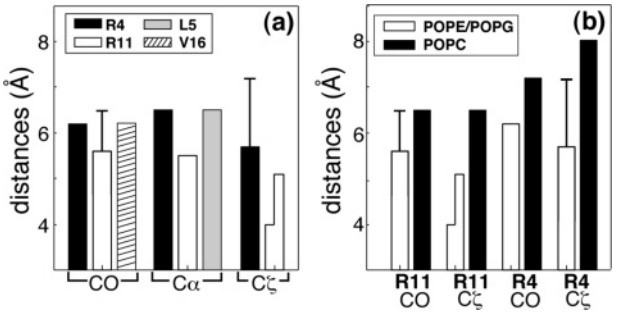

Figure 3. Summary of site-specific $^{13}C-^{31}P$ distances between PG-1 and lipid ^{31}P. (a) Distance comparison for various sites in the POPE/POPG membrane. (b) Comparison of distances between the POPE/POPG membrane (open) and the POPC membrane (filled). "Error" bars indicate distance distributions.

Figure 3 summarizes the $^{13}C-^{31}P$ distances in the POPE/POPG and POPC membranes. Arg_{11} is the closest residue to the lipid headgroups, and the side chain guanidinium Cζ is closer to ^{31}P than the backbone atoms. Both Arg residues lie closer to the phosphates in the anionic membrane than in the zwitterionic membrane.

Arg_4 and Arg_{11} Conformation. To confirm the β-hairpin conformation of PG-1 in the lipid membrane, we determined the backbone (ϕ, ψ) torsion angles of Arg_4 and Arg_{11} using the dipolar correlation experiments HNCH[34] and NCCN.[31,32] Figure 4 shows the HNCH (ϕ angle) and NCCN (ψ angle) data of the two residues in POPC (a, b) and POPE/POPG (c) membranes at 253 K. Both experiments give doubly degenerate angles due to the intrinsically uniaxial nature of the dipolar interaction. This gives rise to $2^4 = 16$ combinations of backbone conformations for each residue. However, using the conformation-dependent Arg Cα and CO chemical shifts (Table 1) and the disulfide bond constraints, we can eliminate most solutions, leaving a single solution of (−120°, 159°) for Arg_4 and (−90°, −75°) for Arg_{11} in the POPC membrane. Root mean-square deviation (rmsd) analysis (Figure S5) gives angular uncertainties of 5°−15°. Thus, Arg_4 adopts a nearly ideal β-strand conformation while Arg_{11} has a β-turn conformation. Changing the membrane to POPE/POPG did not affect the Arg_4 ϕ angle (Figure 4c) but altered the Arg_{11} ϕ angle from −90° to −60°. The larger impact of the lipid headgroup on the Arg_{11} conformation than that of Arg_4 is consistent with the shorter distances of Arg_{11} to the phosphate groups. Figure 5 summarizes the (ϕ, ψ) angles of Arg_4 and Arg_{11} in POPC membranes.

^{1}H Spin Diffusion from the Lipid Chain to the Headgroup in the Liquid−Crystalline Phase. To provide further constraints to the membrane morphology and PG-1 topology in the POPE/POPG membrane, we measured the ^{1}H spin diffusion rates from the lipid chains to the headgroups in the absence and presence of PG-1. A $^{31}P-^1H$ 2D correlation experiment was used, where the chain $(CH_2)_n$ to the ^{31}P cross-peak results from distance-dependent ^{1}H spin diffusion. In the LC phase where the lipid $^1H-^1H$ dipolar coupling is weakened by motion, a lamellar bilayer free of the peptide requires several hundred milliseconds for the $(CH_2)_n-P$ cross-peak to develop.[35] If PG-1 inserts into the hydrophobic part of the membrane, or if PG-1 binding shortens the headgroup−chain distance through chain upturns,[38,39] then spin diffusion will be faster, giving rise to a stronger $(CH_2)_n-P$ cross-peak.

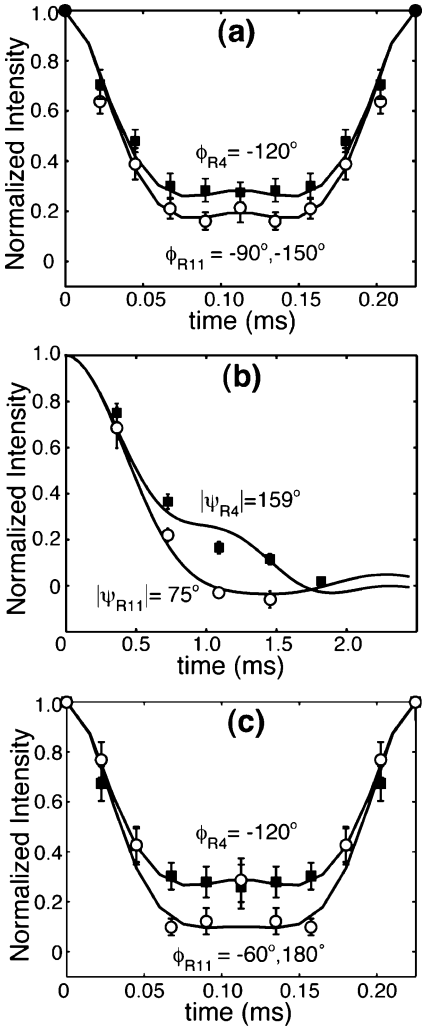

Figure 4. HNCH (a, c) and NCCN (b) data and best-fit simulations of Arg_4 (■) and Arg_{11} (○) in the POPC membrane (a, b) and POPE/POPG membrane (c). (a) The best-fit ϕ angles are −120 ± 15° for Arg_4 and −90 ± 10° for Arg_{11} in the POPC membrane. (b) The best-fit ψ angles are 159 ± 5° for Arg_4 and −75 ± 15° for Arg_{11} in the POPC membrane. (c) The best-fit ϕ angles are −120 ± 15° for Arg_4 and −60 ± 10° for Arg_{11} in the POPE/POPG membrane. The angular uncertainty was estimated from RMSD analyses (Figure S5).

Figure 6 compares the $^{31}P-^1H$ 2D spectra of POPE/POPG membranes without (a, c) and with (b, d) PG-1, measured with a ^{1}H mixing time of 64 ms. Both spectra show the strongest cross-peak from the glycerol G3 and α protons, which are closest to the phosphate group. The ^{1}H chemical shift assignment is obtained from a $^{13}C-^1H$ 2D correlation spectrum shown in the Supporting Information Figure S6. Relative to the largest G3/α cross-peak, the $(CH_2)_n$ cross-peak of the peptide-bound membrane is 3-fold higher than that of the peptide-free sample. Thus, either the chain−headgroup distance is shortened in the presence of PG-1 or PG-1 inserts into the acyl chain region, providing a faster spin diffusion route to the headgroup.

^{1}H Spin Diffusion from Water to Peptide in the Gel Phase. Previous experiments on PG-1 bound to DLPC,[22,25] POPC,[21] and POPE/POPG bilayers[20] showed that the peptide is well inserted into these membranes in the LC phase. To verify that in the gel phase PG-1 remains inserted, we carried out a gel-

(38) Huster, D.; Arnold, K.; Gawrisch, K. *J. Phys. Chem.* **1999**, *103*, 243−251.
(39) Huster, D.; Gawrisch, K. *J. Am. Chem. Soc.* **1999**, *121*, 1992−1993.

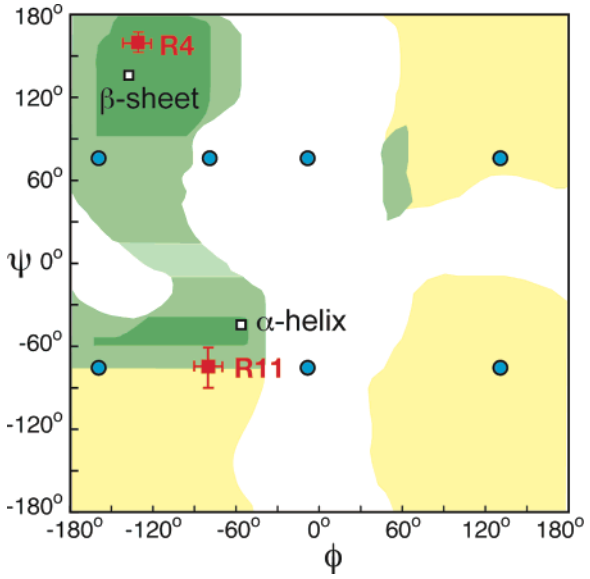

Figure 5. Ramachandran diagram of Arg_4 and Arg_{11} in PG-1. Experimental (ϕ, ψ) torsion angles are shown in red squares. Blue circles indicate other (ϕ, ψ) angle solutions for Arg_{11} that are ruled out by chemical-shift and disulfide-bond constraints. The classical α-helix and β-sheet positions are indicated as open squares.

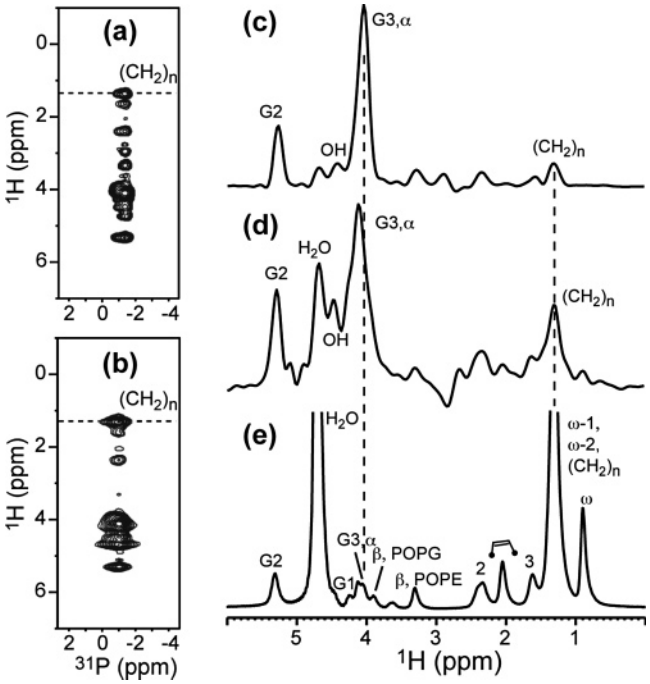

Figure 6. $^{31}P-^{1}H$ correlation spectra of hydrated POPE/POPG membranes with and without PG-1 after a ^{1}H spin diffusion mixing time of 64 ms. (a, b) 2D spectra of POPE/POPG bilayers without and with PG-1, respectively. ^{1}H cross sections are shown in (c) for the peptide-free membrane and (d) for the peptide-bound membrane. (e) Direct-excitation ^{1}H spectrum of the POPE/POPG membrane for comparison. Assignment is obtained from $^{13}C-^{1}H$ 2D correlation (Figure S6). The $(CH_2)_n$ cross-peak in (d) is much higher than that in (c). The low H_2O cross-peak in (c) is attributed to strong hydrogen bonding between the lipid headgroups and water, which immobilizes water and prevents their detection by the ^{1}H T_2 filter. PG-1 likely disrupts some of the lipid−water hydrogen bonds, increasing the H_2O peak intensity in (d).

phase ^{1}H spin diffusion experiment that transfers the water ^{1}H magnetization on the membrane surface to the peptide.[36,37] The depth of individual residues is estimated from the rate of the spin diffusion buildup curves. The experiment was carried out at ~240 K on DLPC-bound PG-1 samples, which had been previously used to measure the insertion state of the peptide in the LC phase.[22] Figure 7 shows the ^{13}C-detected water-to-peptide ^{1}H spin diffusion curves for four residues. Gly_2 Cα and Phe_{12} CO exhibit the fastest buildup curves (a, b), indicating binding to the headgroup and glycerol backbone regions close to the water molecules. Leu_5 Cα and Val_{16} CO show significantly slower initial buildup rates (c, d), which are consistent with insertion to the beginning of the acyl chains. The relative depths are Gly_2 < Phe_{12} < Leu_5 ≈ Val_{16}. This profile is identical to that measured in the LC phase.[22] Thus, freezing the bilayer to the gel phase does not change the insertion state of PG-1.

Discussion

The (ϕ, ψ) torsion angle data shown here indicate that PG-1 adopts an ideal β-strand conformation at Arg_4 and β-turn torsion angles at Arg_{11}, confirming that the peptide has a β-hairpin fold under the solid-state NMR experimental conditions. This rigid disulfide-linked β-hairpin is ~30 Å long based on the solution NMR structure of the peptide.[14]

The $^{13}C-^{31}P$ REDOR distance data indicate that no measured residues in PG-1 are far from the ^{31}P atoms. The distances are 4.0−6.5 Å in the POPE/POPG membrane and 6.5−8.0 Å in the POPC membrane. This close proximity contrasts with the much longer $^{13}C-^{31}P$ distances between the lipid chains and the headgroups. What membrane morphology and peptide topology can give rise to similarly short $^{13}C-^{31}P$ distances for four widely dispersed residues in a β-hairpin?

Figure 8 illustrates three possible scenarios of membrane morphology and peptide insertion states that satisfy the distance data. First, the short distances could result from PG-1 being bound to the lipid bilayer surface (Figure 8a). However, this is inconsistent with various orientation and depth data acquired on a number of lipid membranes. In LC-phase DLPC (12:0) bilayers, PG-1 β-strands were found to be tilted by ~55° from the bilayer normal based on ^{13}C and ^{15}N anisotropic chemical shifts on glass-plate oriented samples.[25] In the longer-chain lipid diphytanoylphosphatidylcholine (DPhPC, 18:0, 22:6), oriented circular dichroism experiments by Huang and co-workers indicated that PG-1 is also transmembrane at peptide−lipid molar ratios larger than ~1:30.[23,40] Since these orientation data were obtained on macroscopically aligned samples, the transmembrane orientation is referenced to the external plane of glass plates, independent of the local curvature of the lipid membrane. In addition to orientation constraints, ^{1}H spin diffusion from the lipid chains to the peptide indicated that PG-1 is in close contact with the acyl chains in both POPC membranes[21] and POPE/POPG membranes[20] in the LC phase, thus the peptide cannot exclusively lie on the membrane surface. The 2D $^{31}P-^{1}H$ spin diffusion spectra shown here confirm the participation of PG-1 in the hydrophobic part of the membrane. Finally, cooling the membrane to the gel phase does not change the depth of insertion of PG-1, since the gel-phase water-to-peptide ^{1}H spin diffusion data gave the same depth profile as the LC-phase Mn^{2+} paramagnetic relaxation enhancement data.[22] Thus, at the peptide−lipid molar ratios used here, PG-1 adopts a stable inserted state in lipid bilayers with varying thicknesses and phases.

(40) Heller, W. T.; Waring, A. J.; Lehrer, R. I.; Harroun, T. A.; Weiss, T. M.; Yang, L.; Huang, H. W. *Biochemistry* **2000**, *39*, 139−145.

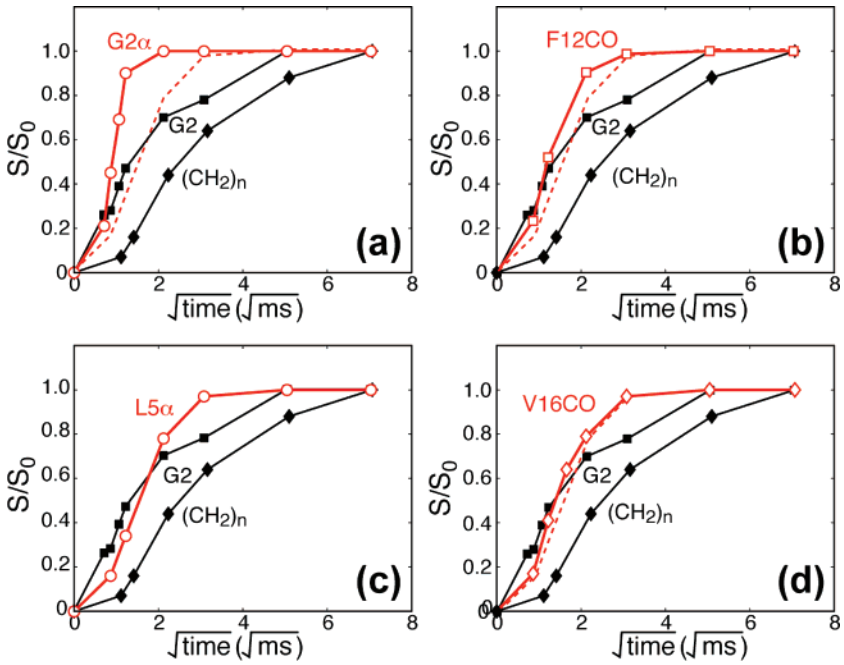

Figure 7. Gel-phase ^{1}H spin diffusion from water to PG-1 in DLPC bilayers at 240 K. Red symbols: Data of ^{13}C-labeled residues in PG-1. Black symbols: data of lipid glycerol G2 and $(CH_2)_n$ signals. The Leu_5 Cα curve is reproduced as dashed lines in (a, b, d) for comparison. The fast buildup of Gly_2 Cα and Phe_{12} CO and the slower buildup curves of Leu_5 Cα and Val_{16} CO are consistent with the paramagnetic relaxation enhancement data on the same samples in the LC phase.[22]

Can the distance data be explained by membrane thinning, where lipid bilayers thin sufficiently to give short distances to all four residues in the peptide (Figure 8b)? This possibility can also be ruled out. Since the thinned membrane remains lamellar, the ^{31}P plane would still be roughly perpendicular to the transmembrane β-strands. This would require Leu_5 Cα and Arg_4 Cα to differ in their $^{13}C-^{31}P$ distances by ~3.6 Å, because the distance between two consecutive α carbons in a β-strand is fixed by the covalent geometry to be 3.6 Å along the β-strand axis. Instead, we measured identical distances of 6.5 Å for Leu_5 Cα and Arg_4 Cα to ^{31}P. Moreover, the fact that short distances are found for backbone as well as the side chain carbons rules out snorkeling of the Arg side chain to the membrane surface.[24,41]

These considerations lead to the conclusion that, for Arg_4 and Leu_5 to have equal Cα−P distances, the local ^{31}P plane must be roughly parallel instead of perpendicular to the β-strand axis. Since the PG-1 β-strands have an externally referenced transmembrane orientation, this parallelity means some lipid molecules must turn their orientation to embed their headgroups in the hydrophobic region of the membrane, thus establishing equidistant contacts to Arg_4 and Leu_5 Cα (Figure 8c). The presence of rotated lipid molecules that merge the two leaflets of lamellar bilayers is the key signature of the toroidal pore.[42,43]

This toroidal pore model is strongly supported by static ^{31}P lineshapes of POPC/POPG, POPE/POPG, and POPC membranes in the presence of PG-1. Both glass-plate aligned samples[44,45] and unoriented liposome samples[25] give rise to spectra with a prominent broad peak centered at the isotropic shift, indicating the presence of nonlamellar lipids with near isotropic morphology. On the other hand, the remaining aligned peak or powder intensity in these spectra indicates that a residual lamellar bilayer remains in these samples, as required by the toroidal pore model; thus complete micelle formation is unlikely.

How can the β-strands lie close to both the headgroups and the acyl chains, as constrained by the $^{13}C-^{31}P$ distances and the lipid-to-peptide ^{1}H spin diffusion data? We hypothesize that the rotated lipid molecules may partially intercalate between the β-strands, such that both the headgroups and the acyl chains are in close contact to the β-strands (Figure 8c). 2D $^{13}C-^{13}C$ correlation spectra of fibrilized PG-1 indicate that the N-strand−N-strand interface is more loosely packed than the C-strand−C-strand interface,[46,47] which may allow lipid intercalation.

Similar to the case for PG-1, short peptide−headgroup distances, short peptide−lipid chain distances, and enhanced lipid headgroup−chain contacts were reported for an α-helical magainin analogue, K3, which contains no Arg but only Lys as its cationic residues.[48] Intriguingly, the short peptide−headgroup distances occur only for ~30% of K3, as manifested by the plateau value of the REDOR curves. This contrasts with the 100% REDOR dephasing of PG-1. The ^{31}P line shapes of the K3-containing membrane also do not exhibit disorder. Thus, the Arg-cationic PG-1 has a stronger membrane-disruptive ability and shorter distances to lipids than the Lys-cationic K3.

The $^{13}C-^{31}P$ distance data of PG-1 not only point to the toroidal pore as the only possible lipid organization near the peptide but also suggest that guanidinium−phosphate association may be the driving force for toroidal pore formation: the Arg

(41) Strandberg, E.; Morein, S.; Rijkers, D. T. S.; Liskamp, R. M. J.; vanderWel, P. C. A.; Killian, J. A. *Biochemistry* **2002**, *41*, 7190−7198.
(42) Matsuzaki, K. *Biochim. Biophys. Acta* **1998**, *1376*, 391−400.
(43) Ludtke, S. J.; He, K.; Heller, W. T.; Harroun, T. A.; Yang, L.; Huang, H. W. *Biochemistry* **1996**, *35*, 13723−13728.
(44) Mani, R.; Buffy, J. J.; Waring, A. J.; Lehrer, R. I.; Hong, M. *Biochemistry* **2004**, *43*, 13839−48.
(45) Mani, R.; Waring, A. J.; Lehrer, R. I.; Hong, M. *Biochim. Biophys. Acta* **2005**, *1716*, 11−18.
(46) Tang, M.; Waring, A. J.; Hong, M. *J. Am. Chem. Soc.* **2005**, *127*, 13919−13927.
(47) Mani, R.; Tang, M.; Wu, X.; Buffy, J. J.; Waring, A. J.; Sherman, M. A.; Hong, M. *Biochemistry* **2006**, *45*, 8341−9.
(48) Toke, O.; Maloy, W. L.; Kim, S. J.; Blazyk, J.; Schaefer, J. *Biophys. J.* **2004**, *87*, 662−74.

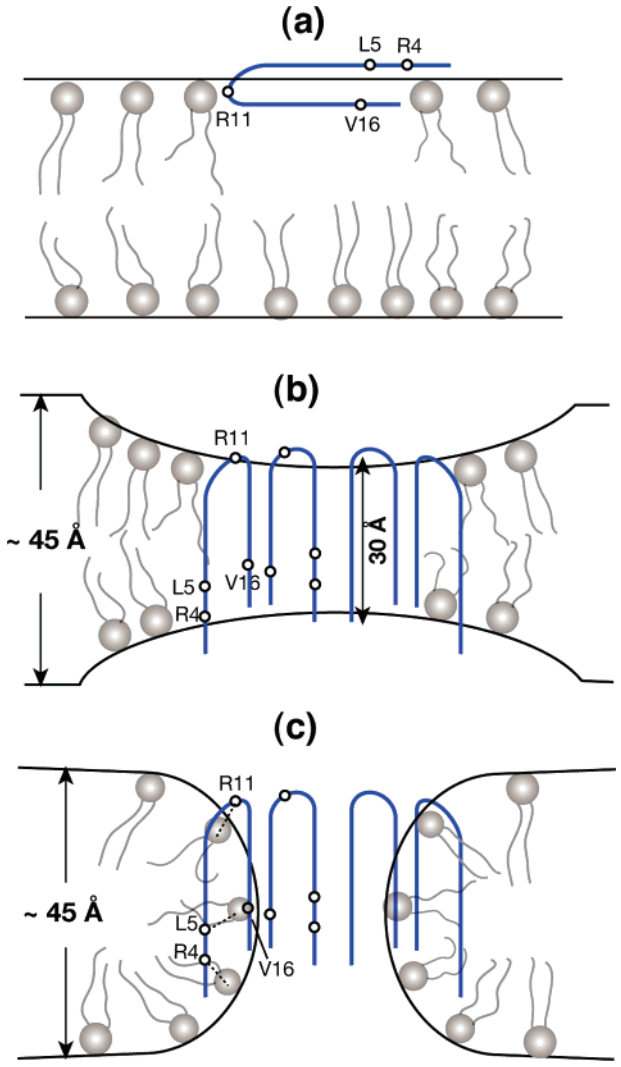

Figure 8. Schmatic structural models of PG-1 in the POPE/POPG membrane. (a) PG-1 is bound to the membrane surface. This model can be ruled out by absolute orientation measurements and ^{1}H spin diffusion data. (b) Peptide oligomers thin the membrane without changing the lipid orientation. Leu$_5$ Cα and Arg$_4$ Cα should differ in their ^{13}C−^{31}P distances by 3.6 Å, which disagrees with the REDOR data. (c) Peptide oligomers cause toroidal pores in the membrane, so that the local ^{31}P plane is roughly parallel to the β-strands, giving rise to similar ^{13}C−^{31}P distances to those for Leu$_5$ Cα and Arg$_4$ Cα. In models (b) and (c), only part of the β-barrel is drawn for clarity.

residues may drag the phosphate groups along to overcome the free energy barrier of insertion into the hydrophobic part of the membrane. This anion-mediated translocation of guanidinium groups has been reported for oligoarginines from water to chloroform and from water to anionic lipid bilayers.[49] Comparisons of different counterions' abilities for polyarginine translocation revealed that a combination of amphiphilic phosphate anions such as the phosphatidylglycerol lipids and hydrophilic phosphates maximizes the translocation across the membrane.[50]

The nature of the guanidinium−phosphate interaction is ionic. This is supported by the 1.0−2.5 Å shorter C−P distances in the anionic POPE/POPG membrane than in the zwitterionic POPC membrane. The cationic trimethylamine group in the

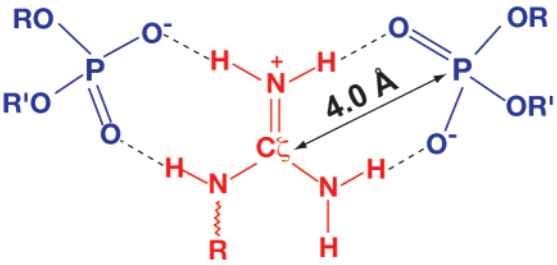

Figure 9. Guanidinium-phosphate bidentate complex, stabilized by multiple hydrogen bonds and electrostatic attraction.

POPC headgroup should repel the guanidinium cation, weakening the guanidinium-phosphate complex. The ionic interaction is also supported by the 1.0−2.0 Å shorter distances of Arg$_{11}$ to ^{31}P than those of Arg$_4$. Arg$_{11}$ is one of three consecutive Arg's at the β-turn and thus belongs to a much larger charge cluster than Arg$_4$, which is surrounded by hydrophobic residues. Thus, electrostatic attraction between guanidinium cations and phosphate anions play an important role in peptide insertion and membrane defect formation.

A second possible contribution to stable guanidinium−phosphate complexation is hydrogen bonding. In the absence of steric hindrance, the guanidinium ion can form as many as four hydrogen bonds with two phosphate groups.[51] This bidentate complex (Figure 9) is unstable for the basic lysine, which may explain the relative abundance of Arg over Lys in cationic AMPs. The short Arg$_{11}$ Cζ−P distances of 4.0 Å and 5.1 Å strongly suggest the existence of such a bidentate complex.

We hypothesize that this ionic and hydrogen-bond-stabilized guanidinium−phosphate complexation may be a general mechanism for the translocation of Arg residues in membrane peptides and proteins, and the resulting membrane defect may be quite common. For example, the Arg-rich TAT(48−60) peptide induces rod-shaped lipid micelles in DMPC membranes.[52] The Arg-rich cyclic defensin RTD-1 causes micron-diameter lipid cylinders.[53] In KvAP potassium channel, the Arg-rich S4 segment is reported to move by ∼20 Å across the membrane during channel opening.[54] MD simulations of the S4 helix suggests that the organization of POPC bilayers is highly perturbed in the vicinity of the helix, with a hydrogen-bonded network of water and phosphate groups formed around the guanidinium ions.[12] Such lipid counterions are shown experimentally here for PG-1. They shield the guanidinium ion from the lipid acyl chains, thus reducing the free energy of membrane insertion.[11]

One difference between PG-1 and other transmembrane cationic proteins is its β-sheet conformation, which promotes oligomerization through backbone N−H···O=C hydrogen bonds.[20,47] This self-assembly may further facilitate the insertion of multiple Arg's by reducing the lipid chain−peptide interface.

Conclusion

The first measurement of the distances between Arg residues in a cationic membrane peptide and the ^{31}P of lipid headgroups

(49) Sakai, N.; Takeuchi, T.; Futaki, S.; Matile, S. *ChemBioChem* **2005**, *6*, 114−122.
(50) Sakai, N.; Matile, S. *J. Am. Chem. Soc.* **2003**, *125*, 14348−14356.
(51) Schug, K. A.; Lindner, W. *Chem. Rev.* **2005**, *105*, 67−114.
(52) Afonin, S.; Frey, A.; Bayerl, S.; Fischer, D.; Wadhwani, P.; Weinkauf, S.; Ulrich, A. S. *ChemPhysChem* **2006**, *7*, 2134−2142.
(53) Buffy, J. J.; McCormick, M. J.; Wi, S.; Waring, A.; Lehrer, R. I.; Hong, M. *Biochemistry* **2004**, *43*, 9800−9812.
(54) Jiang, Y.; Ruta, V.; Chen, J.; Lee, A.; MacKinnon, R. *Nature* **2003**, *423*, 42−48.

is presented. The uniformly short $^{13}C-^{31}P$ distances for multiple sites in PG-1 indicate that the β-hairpin peptide induces toroidal pores in the membrane, where some lipid headgroups become embedded in the hydrophobic region of the bilayer. Comparison of distances in anionic membranes and zwitterionic membranes suggests that the driving force for the toroidal pore formation is guanidinium−phosphate association, which neutralizes the guanidinium ions to facilitate their insertion into the hydrophobic part of the membrane. Thus, PG-1 may pull the phosphate groups along as it inserts, causing toroidal pores. We propose that this guanidinium−phosphate complexation may be a general phenomenon among membrane-lytic Arg-rich antimicrobial peptides.

Acknowledgment. This work is supported by the National Institutes of Health Grants GM-066976 to M.H. and AI-37945 to A.J.W.

Supporting Information Available: Description of the multispin simulations, additional spectra and control distance data, rmsd analysis for the torsion angle data, and 2D $^{1}H-^{13}C$ spectrum of lipids for assignment are provided. This material is available free of charge via the Internet at http://pubs.acs.org.

JA072511S